

ChemComm

Accepted Manuscript



This is an *Accepted Manuscript*, which has been through the Royal Society of Chemistry peer review process and has been accepted for publication.

Accepted Manuscripts are published online shortly after acceptance, before technical editing, formatting and proof reading. Using this free service, authors can make their results available to the community, in citable form, before we publish the edited article. We will replace this *Accepted Manuscript* with the edited and formatted *Advance Article* as soon as it is available.

You can find more information about *Accepted Manuscripts* in the [Information for Authors](#).

Please note that technical editing may introduce minor changes to the text and/or graphics, which may alter content. The journal's standard [Terms & Conditions](#) and the [Ethical guidelines](#) still apply. In no event shall the Royal Society of Chemistry be held responsible for any errors or omissions in this *Accepted Manuscript* or any consequences arising from the use of any information it contains.

COMMUNICATION

Highly dispersed Fe₂O₃ on carbon nanotubes for low-temperature selective catalytic reduction of NO with NH₃

Cite this: DOI: 10.1039/x0xx00000x

Received 00th January 2012,
Accepted 00th January 2012Zhenping Qu^{*a}, Lei Miao^a, Hui Wang^a, Qiang Fu^b

DOI: 10.1039/x0xx00000x

www.rsc.org/

The highly dispersed Fe₂O₃ nanoparticles supported on carbon nanotubes, prepared by a simple ethanol-assisted impregnation method, showed above 90% NO conversion and selectivity at low temperatures (200-325°C). Moreover the excellent SO₂/H₂O durability and stability were obtained.

Nitrogen oxides (NO_x) have given rise to a variety of increasing harmful impact on the environment. Nowadays, selective catalytic reduction (SCR) with NH₃ has been proven to be the most effective technology. The typical commercial V₂O₅-WO₃ (MoO₃)/TiO₂ catalysts reveal the adequate catalytic activity at 300-400°C. However, it is still not satisfactory with respect to the toxicity of vanadium, the easy deactivation and the poor low-temperature catalytic activity. Therefore, extensive studies have been performed to develop the new SCR catalysts which can substitute the V-based catalysts. Among them, iron oxides catalysts with low cost have received much attention due to their environmentally benign character and good thermal stability in many reactions, such as oxidation of CO, Fischer-Tropsch synthesis reaction, photocatalysis etc. However the predominant activity for SCR was mainly in middle and high temperature ranges (250-500°C)¹. Only 80 % NO conversion was obtained from 200 to 400°C on γ-Fe₂O₃ nanorods, moreover SO₂ and H₂O had a negative impact on the catalytic performance². The poor low-temperature activity and SO₂ resistance became the main restrictive factors for their application^{3,4}. No enough active sites to activate NH₃ over γ-Fe₂O₃ nanorods and/or low activation ability should be the main reason for the lower activity. Hence, it is very urgent to enhance the low-temperature SCR activity and SO₂ resistance of iron oxide catalyst.

Some researchers have used suitable supports to improve low-temperatures SCR performance of iron oxides, such as Fe/BEA⁵, Fe/ZSM-5⁶ and Fe₂O₃/TiO₂⁷. But low-temperature activity was still unsatisfactory. Recently, carbon nanotubes (CNTs) were attracting more and more attention due to their excellent stabilities, unique electronic and structural properties⁸. CNTs had an outstanding combination of mechanical strength and stiffness, electrical and thermal conductivity, and low density, making them promising catalytic supports. Chen et al.⁹ found the confinement effect in CNTs could effectively enhance Fischer-Tropsch catalytic performance and affect the size of nanoparticles. Jiang et al.¹⁰ prepared Co₃O₄/CNTs

for the catalytic combustion of toluene and it reached the completed conversion at 257°C. While for SCR studies, the enhancement of SCR activity has also been observed when metal oxides were supported on CNTs, especially in the low temperature ranges. Zhang et al.¹¹ have tried to prepare Fe₂O₃/CNTs, but the SCR activity was still less than 80% below 250°C. In addition, SO₂ poisoned their Fe₂O₃/CNTs catalyst and 8% NO conversion decrease was observed in the present of 200 ppm SO₂. Moreover the effects of CNTs on iron oxides and their interaction were still unclear.

Now, the control of the dispersion of metal oxides on the surface of CNTs was still very essential for the activity enhancement. In this communication, it was the first time to report the highly dispersed Fe₂O₃/CNTs nanoparticles prepared by a simple ethanol-assisted impregnation method for NO_x SCR. And the pure Fe₂O₃ was also employed by a direct calcination method for comparison (Experimental Section in Supporting Information). The catalytic performance of Fe₂O₃/CNTs catalysts in the selective catalytic reduction of ammonia (SCR) was studied in a fixed-bed flow reactor (8 mm in interior diameter). The composition and amount of the inlet gas mixture was set by mass flow controllers. The typical reactant gas composition was as follows: 1000 ppm NH₃, 1000 ppm NO, 3 vol% O₂, and balance N₂. The total flow rate of the reaction mixture was 300 ml/min, corresponding to a GHSV of 30000 h⁻¹. NO_x concentration was monitored by an NO-NO₂-NO_x analyzer (Thermo Scientific 42i-HL). N₂ was detected by a gas chromatograph (GC 7890T, Techcomp, China). In order to ensure the accuracy, all experiments were repeated three times at least.

CNTs provided a large surface area (Table 1), which was an important advantage and nature as a support. After the addition of Fe₂O₃, the surface area of Fe₂O₃/CNTs was found to be slightly increased, while the pore volume and pore size were significantly

Table 1 The physical characteristics of CNTs and Fe₂O₃/CNTs catalysts

Samples	BET Surface area (m ² /g)	Pore volume (cm ³ /g)	Pore size (nm)
Raw CNTs	152.8	1.74	45.42
Treated CNTs	163.1	1.74	42.61
Fe ₂ O ₃ /CNTs	176.1	0.44	10.08
Pure Fe ₂ O ₃	27.36	0.18	3.09

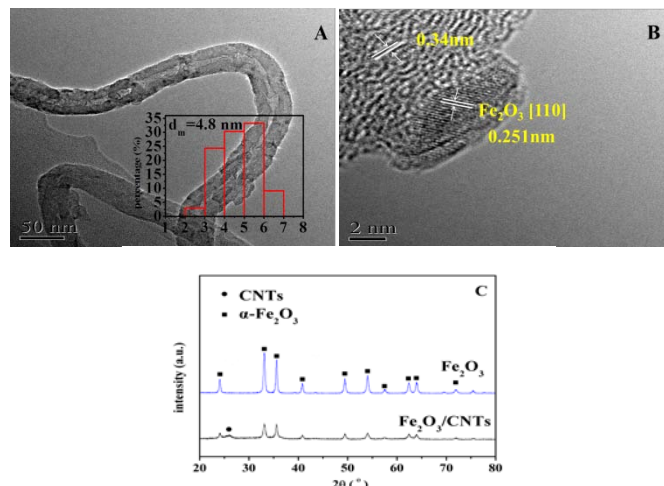


Fig. 1 HRTEM images of $\text{Fe}_2\text{O}_3/\text{CNTs}$ (A, B) and XRD patterns (C) of catalysts.

decreased. Parts of Fe_2O_3 entered into channels of CNTs and formed highly dispersed nanoparticles¹². The slight increase in the surface area should be due to the the formation of the interparticle pores. The TEM images of $\text{Fe}_2\text{O}_3/\text{CNTs}$ (Fig. 1(A)) also gave the strong support that the high dispersion of Fe_2O_3 nanoparticles with the mean particle size of 4.8 nm have been obtained. Meanwhile, some Fe_2O_3 nanoparticles were also observed inside the CNT channels. The good wetting and spreading behavior of ethanol benefited for the dispersion of CNTs and metal oxide particles. And the low surface tension, low viscosity and low surface resistance of ethanol effectively facilitated the introduction of metal oxides to walls of CNTs^{13,14}. These nanoparticles on the CNTs exhibited a d spacing of 0.251 nm, corresponding to the [110] plane of $\alpha\text{-Fe}_2\text{O}_3$ nanoparticles, as shown in the HRTEM image (Figure 1(B)). On the other hand, the characteristic diffraction peaks of $\alpha\text{-Fe}_2\text{O}_3$ were also clearly observed for the catalyst in the XRD patterns (Fig. 1(C)). Compared with pure $\alpha\text{-Fe}_2\text{O}_3$, the $\text{Fe}_2\text{O}_3/\text{CNTs}$ catalyst showed the good dispersion of $\alpha\text{-Fe}_2\text{O}_3$ nanoparticles (Fig. 1(C)).

The interaction and redox behavior of CNT supported Fe_2O_3 catalysts were investigated by XPS, H_2 -TPR and NH_3 -TPD analyses. Fig. 2(A) showed the Fe 2p core-level binding energy spectrum of the catalysts. The fitting peaks at around 710 eV and 723 eV could

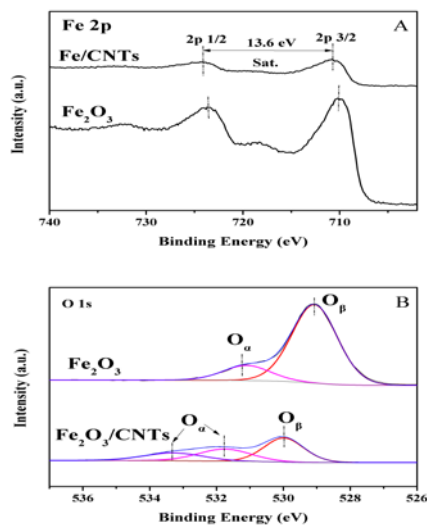


Fig. 2 XPS spectra of Fe 2p (A) and O 1s (B) for $\text{Fe}_2\text{O}_3/\text{CNTs}$ and Fe_2O_3 catalysts.

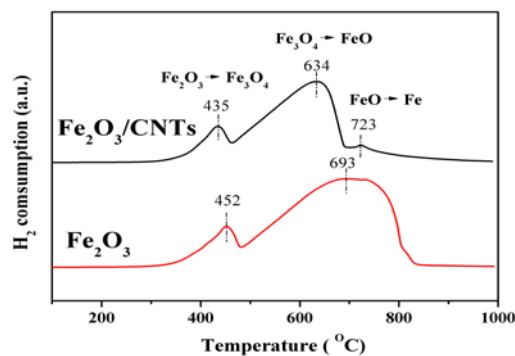


Fig. 3 H_2 -TPR profiles of Fe_2O_3 and $\text{Fe}_2\text{O}_3/\text{CNTs}$ catalysts.

be assigned to $\text{Fe}2p_{3/2}$ and $\text{Fe} 2p_{1/2}$ peaks, respectively. The separation of the 2p doublet was 13.6 eV. All these features were typical of Fe_2O_3 . The binding energy (BE) of Fe 2p for the $\text{Fe}_2\text{O}_3/\text{CNTs}$ was found to be a slightly higher value compared with pure Fe_2O_3 , which indicated that CNTs strongly influenced the oxidation (electronic) state of the Fe_2O_3 nanoparticles¹⁵. The XPS spectra of O 1s for catalysts were displayed in Fig. 2(B). The O 1s XPS spectra were fitted into two peaks assigned to the lattice oxygen at low binding energy (529.06-529.9 eV) and the surface-adsorbed oxygen at high binding energy (531.1-533.2 eV), which was donated as O_β and O_α , respectively¹⁴. Compared with the O_β peak of pure Fe_2O_3 catalyst, the O_β peaks shifted to a higher binding energy when Fe_2O_3 was supported on CNTs. This peak shift also suggested the existence of an interaction between lattice oxygen and Fe atoms, which would result in an easy transfer of lattice oxygen atom to the surface of catalyst¹⁶. On the other hand, the redox peaks of $\text{Fe}_2\text{O}_3/\text{CNTs}$ shifted to the lower temperature in contrast with pure Fe_2O_3 (Fig. 3). Transition metals were well-known to interact with graphite through hybridization of orbitals, and the confinement effect of CNTs actuated a considerable interaction between metal oxide and CNTs¹⁶. The $\alpha\text{-Fe}_2\text{O}_3$ supported on CNTs was easily to be reduced, and the oxygen in the catalyst was more active, which revealed that the unique electronic properties of CNTs could promote charge transfer between iron atoms and CNTs, leading to the enhancement in its redox potential¹⁵. In addition, the enhanced NH_3 adsorption could only be clearly detected on $\text{Fe}_2\text{O}_3/\text{CNTs}$ in NH_3 -TPD experiment compared with pure Fe_2O_3 and CNTs, which indicated that CNTs promoted NH_3 adsorption and activation on the surface of Fe_2O_3 . The enhanced electron transfer ability between Fe_2O_3 and CNT would play a vital role in low-temperature reaction.

The NH_3 -SCR activity, $\text{SO}_2/\text{H}_2\text{O}$ resistance ability and stability of the catalysts were shown in Fig. 4. Pure Fe_2O_3 showed low activity and only 55% NO conversion was obtained when the temperature reached 275°C. It should be noted that the introduction of CNTs as supports caused a significant improvement of NO conversion over the catalyst, which suggested that the interaction between Fe_2O_3 and

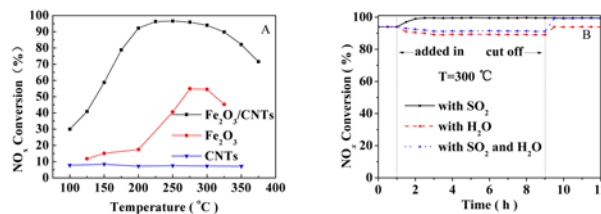


Fig. 4 NO_x conversion as a function of temperature over different catalysts (A) and SO_2 tolerance of $\text{Fe}_2\text{O}_3/\text{CNTs}$ catalyst (B).

CNTs was important for the SCR reaction. T_{50} for NH_3 -SCR reaction on $\text{Fe}_2\text{O}_3/\text{CNTs}$ catalyst was below 150°C and the maximum NO conversion was 96.6% at 250°C . The temperature ranged for 90% NO conversion ranges from 200 to 325°C . The N_2 selectivity was maintained at above 90% over the whole temperature range (Fig. S1) and only N_2O was the main by-product. In addition, CNTs did not participate in the reaction as a reducing agent and no CO or CO_2 was detected. This salient performance was of utmost importance in NO_x removal at low temperatures ($<250^\circ\text{C}$). Traditional iron oxides catalysts were proved to be suitable for SCR in the middle and high temperature (250 - 500°C). In recent studies, some researchers have paid attention to composite oxides and supported catalysts. However, the NO conversion at low temperatures ($<250^\circ\text{C}$) had not evidently improved yet. Liu et al.¹⁷ found that Fe- β catalysts showed less than 70% NO conversion below 250°C . Yang et al.¹⁸ studied that $\text{V}_2\text{O}_5/\text{Fe}_2\text{O}_3\text{-TiO}_2$ catalysts revealed less than 80% NO conversion below 250°C . Shwan et al.¹⁹ discovered that Fe-BEA catalysts exhibited less than 60% NO conversion below 250°C . Compared with previous studies, we achieved a breakthrough in NO conversion at low temperatures.

According to the XPS results (Fig. 2(B)), the relative concentration ratios of $\text{O}_\alpha/(\text{O}_\alpha+\text{O}_\beta)$ for $\text{Fe}_2\text{O}_3/\text{CNTs}$ and pure Fe_2O_3 were calculated to be 0.53, and 0.17, respectively. It has been known that the formation of O_α was helpful for adsorption and transformation of NH_3 on the surfaces of catalysts, which should be one of the reasons that $\text{Fe}_2\text{O}_3/\text{CNTs}$ presented the excellent catalytic activity. On the other hand, high dispersion could improve the interaction between metal oxides and CNTs and facilitate adsorption of reactant gas on the active sites of catalysts. Activated carbon has also been used to support Fe_2O_3 in our study. No interaction between activated and Fe_2O_3 was observed (Fig. S2), and only 73% NO conversion at 250°C was obtained. Therefore, especially in the low temperature ranges, CNTs strongly promoted the catalytic activity of iron oxides due to its unique electronic properties and the interaction with oxides. Moreover the $\text{Fe}_2\text{O}_3/\text{CNTs}$ catalyst deactivation was not observed during the whole test period at 250°C under GHSV of 30000 h^{-1} and 60000 h^{-1} (Fig. S3), and the dispersity of Fe_2O_3 nanoparticles was not changed after a 48 h continuous running reaction (Fig. S4).

As the exhaust usually comprised a certain amount of SO_2 and H_2O , the $\text{Fe}_2\text{O}_3/\text{CNTs}$ catalyst with a feed stream containing 200 ppm SO_2 and 10 vol% H_2O at a typical temperature (300°C) were tested. As shown in Fig. 4(B), the NO conversion increased gradually with SO_2 introduction. After eliminating SO_2 , the NO conversion remained unchanged. The promoting effect of SO_2 was investigated by NH_3 -TPD (Fig. S5). It was found that the intensity of NH_3 desorption for sulfated $\text{Fe}_2\text{O}_3/\text{CNTs}$ catalyst became stronger than the fresh $\text{Fe}_2\text{O}_3/\text{CNTs}$ sample. The presence of SO_2 increased the acid sites for NH_3 adsorption and activation on the catalyst surface, which promoted the SCR activity. The $\text{Fe}_2\text{O}_3/\text{CNTs}$ catalyst also displayed good H_2O resistance (Fig. 4(B)). When removing H_2O , the SCR activity could recover rapidly. Meanwhile, in the co-existence of SO_2 and H_2O , the $\text{Fe}_2\text{O}_3/\text{CNTs}$ catalyst also displayed high NO conversion (more than 90% at 300°C). The fairly excellent activity and stability of $\text{Fe}_2\text{O}_3/\text{CNTs}$ catalyst predicted an attractive prospect for the practical applications.

Conclusions

In summary, highly dispersed $\text{Fe}_2\text{O}_3/\text{CNTs}$ catalyst was prepared by a simple ethanol-assisted impregnation method, and Fe_2O_3 nanoparticles with the mean particle size of 4.8 nm were obtained. The redox property of iron oxides, adsorption and activation ability of nitrogen oxides were effectively

improved due to the excellent electron transfer property of CNTs. More than 90% NO conversion was achieved from 200 to 325°C , which was attributed to the large surface area, fine dispersion of $\alpha\text{-Fe}_2\text{O}_3$ and the interaction with CNTs. It was also found that SO_2 promoted the SCR activities and $\text{Fe}_2\text{O}_3/\text{CNTs}$ catalyst showed excellent $\text{SO}_2/\text{H}_2\text{O}$ resistance and reaction stability.

Notes and references

* Corresponding author

^a Key Laboratory of Industrial Ecology and Environmental Engineering (MOE), School of Environmental Science and Technology, Dalian University of Technology, Linggong Road 2, Dalian 116024, China.

^b State Key Laboratory of Catalysis, Dalian Institute of Chemical Physics, Chinese Academy of Sciences, Dalian 116023, China.

† Electronic Supplementary Information (ESI) available: Experimental section, Catalyst characterization, N_2 selectivity and stability. See DOI: 10.1039/c000000x/

- 1 F. Liu, H. He and C. Zhang, *Chemical Communications*, 2008, 2043-2045.
- 2 X. Mou, B. Zhang, Y. Li, L. Yao, X. Wei, D. S. Su, and W. Shen, *Angew. Chem. Int. Ed.*, 2012, **51**, 2989-2993.
- 3 F. Liu, H. He, Z. Lian, W. Shan, L. Xie, K. Asakura, W. Yang and H. Deng, *Journal of Catalysis*, 2013, **307**, 340-351.
- 4 F. Liu, H. He, C. Zhang, Z. Feng, L. Zheng, Y. Xie and T. Hu, *Applied Catalysis B: Environmental*, 2010, **96**, 408-420.
- 5 R. Nedyalkova, S. Shwan, M. Skoglundh and L. Olsson, *Applied Catalysis B: Environmental*, 2013, **138-139**, 373-380.
- 6 T. Du, H. Qu, Q. Liu, Q. Zhong, W. Ma, *Chemical Engineering Journal*, DOI: 10.1016/j.cej.2014.09.119
- 7 F. Liu and H. He, *Journal of Physical Chemistry C*, 2010, **114**, 16929-16939
- 8 X. Pan and X. Bao, *Chemical Communications*, 2008, 6271-6281.
- 9 W. Chen, Z. Fan, X. Pan and X. Bao, *Journal of the American Chemical Society*, 2008, **130**, 9414-9419.
- 10 S. Jiang and S. Song, *Applied Catalysis B: Environmental*, 2013, **140-141**, 1-8.
- 11 J. Han, D. Zhang, P. Maitarad, L. Shi, S. Cai, H. Li, L. Huang and J. Zhang, *Catalysis Science & Technology*, 2014, DOI: 10.1039/c4cy00789a.
- 12 R. M. M. Abbaslou, J. Soltan and A. K. Dalai, *Applied Catalysis A: General*, 2010, **379**, 129-134.
- 13 J. S. Hong, J. H. Lee and Y. W. Nam, *Carbon*, 2013, **61**, 577-584.
- 14 Y. Su, B. Fan, L. Wang, Y. Liu, B. Huang, M. Fu, L. Chen and D. Ye, *Catalysis Today*, 2013, **201**, 115-121.
- 15 J. r. Radnik, C. Mohr and P. Claus, *Physical Chemistry Chemical Physics*, 2003, **5**, 172-177.
- 16 L. Chen, J. Li and M. Ge, *The Journal of Physical Chemistry C*, 2009, **113**, 21177-21184.
- 17 H. Liu, J. Wang, T. Yu, S. Fan and M. Shen, *Catalysis Science & Technology*, 2014, **4**, 1350-1356.
- 18 S. Yang, C. Wang, L. Ma, Y. Peng, Z. Qu, N. Yan, J. Chen, H. Chang and J. Li, *Catalysis Science & Technology*, 2013, **3**, 161-168.
- 19 S. Shwan, J. Jansson, L. Olsson and M. Skoglundh, *Catalysis Science & Technology*, 2014, **4**, 2932-2937.